Chicken gga-miR-103-3p Targets CCNE1 and TFDP2 and Inhibits MDCC-MSB1 Cell Migration

Bo Han,*,1 Ling Lian,*,1 Xin Li,* Chunfang Zhao,* Lujiang Qu,* Changjun Liu,† Jiuzhou Song,‡ and Ning Yang*,2

*Department of Animal Genetics and Breeding, National Engineering Laboratory for Animal Breeding, College of Animal Science and Technology, China Agricultural University, Beijing 100193, China, †Division of Avian Infectious Diseases, Harbin Veterinary Research Institute of Chinese Academy of Agricultural Sciences, Harbin 150001, China, and ‡Department of Animal and Avian Sciences, University of Maryland, College Park, Maryland 20742

ABSTRACT Marek's disease (MD) is a highly contagious viral neoplastic disease caused by Marek's disease virus (MDV), which can lead to huge economic losses in the poultry industry. Recently, microRNAs (miRNAs) have been found in various cancers and tumors. In recent years, 994 mature miRNAs have been identified through deep sequencing in chickens, but only a few miRNAs have been investigated further in terms of their function. Previously, gga-miR-103-3p was found downregulated in MDV-infected samples by using Solexa deep sequencing. In this study, we further verified the expression of gga-miR-103-3p among MDV-infected spleen, MD lymphoma from liver, noninfected spleen, and noninfected liver, by qPCR. The results showed that the expression of gga-miR-103-3p was decreased in MDV-infected tissues, which was consistent with our previous study. Furthermore, two target genes of gga-miR-103-3p, cyclin E1 (*CCNE1*) and transcription factor Dp-2 (E2F dimerization partner 2) (*TFDP2*), were predicted and validated by luciferase reporter assay, qPCR, and western blot analysis. The results suggested that *CCNE1* and *TFDP2* are direct targets of gga-miR-103-3p in chickens. Subsequent cell proliferation and migration assay showed that gga-miR-103-3p suppressed MDCC-MSB1 migration, but did not obviously modulate MDCC-MSB1 cell proliferation. In conclusion, gga-miR-103-3p targets the *CCNE1* and *TFDP2* genes, and suppresses cell migration, which indicates that it might play an important role in MD tumor transformation.

Marek's disease (MD) is a highly contagious T-cell lymphoid neoplasia of chickens induced by an alphaherpesvirus, gallid herpesvirus type 2 (GaHV-2), which is historically known as Marek's disease virus (MDV) (Gennart *et al.* 2015). MDV infection can be generally divided into four phases: early cytolytic, latent, late cytolytic, and tumor transformation phase (Calnek 2001). The disease is characterized by monocyte infiltration, and the formation of tumor lesions in chickens peripheral nerves, gonad, iris, various organs, muscles, skin, and other tissues (Calnek 1986, 2001), which causes huge economic losses to the poultry industry. Currently, MD can be prevented by virus vaccine, which is injected into 1-d-old chickens. However, the efficacy of the vaccine has decreased concomitantly with the increase in virulence of MDV (Gimeno 2008). Therefore, it is important to explore better approaches to control this disease, for which investigating the mechanism of resistance, and the susceptibility of chickens, will be among the most important strategies.

MicroRNAs (miRNAs) are small, noncoding, endogenous single-strand RNA molecules of 21–26 nt, which repress gene expression by binding to complementary sequences in the 3′-untranslated region (3′-UTR) of mRNAs to prevent their translation (Bartel 2009). miRNAs are also involved in multiple cellular processes, including cell proliferation, migration, and apoptosis (Wang *et al.* 2010). Extensive studies on miRNAs have been carried out in human cancers (Calin and Croce 2006; Farazi *et al.* 2013; Iorio and Croce 2012; Lu *et al.* 2005). In chickens, miRNAs have been studied, and the roles they play in growth performance, reproduction, and disease resistance have been elucidated

■ **Table 1 Real-time PCR primers for detecting expression of gga-miR-103-3p**

miRNA	Direction[a]	Sequence
gga-miR-103-3p	Forward	AGCAGCATTGTACAGGGCTATGAA
Chicken 5S rRNA[b]	Forward	ACCGGGTGCTGTAGGCTTAA

[a] The universal reverse primer was provided by the kit of miRACLE qPCR miRNA Master Mix (Genetimes Technology, Shanghai, China).
[b] 5S rRNA acted as a reference.

(Burnside and Morgan 2011; Wang *et al.* 2013; Han *et al.* 2015; Li *et al.* 2012, 2013; Lin *et al.* 2012; Kang *et al.* 2013; Rengaraj *et al.* 2013; X. Wang *et al.* 2014; Zhang *et al.* 2013). The chicken and MDV-encoded miRNAs were first identified in MDV-infected chicken embryo fibroblasts (CEF) by Burnside *et al.* (2006). Since then, many viral miRNAs had been found, and are considered to play critical roles in MDV tumorigenesis (Morgan *et al.* 2008; Zhao *et al.* 2009, 2011; Luo *et al.* 2011; Xu *et al.* 2011; Hicks and Liu 2013; Z. Li *et al.* 2014; Yu *et al.* 2014; Chi *et al.* 2015; Teng *et al.* 2015). However, the functions of host miRNAs involved in chicken MD still need to be investigated (Burnside *et al.* 2008; Lian *et al.* 2012a, 2012b, 2015; Tian *et al.* 2012; X. Li *et al.* 2014).

In a previous study (Lian *et al.* 2012a), we identified 187 known chicken miRNAs in MDV-infected samples by Solexa deep sequencing, among which, gga-miR-103-3p was downregulated in MDV-infected groups. In this study, we further verified its targets and conducted a preliminarily investigation into the role of gga-miR-103-3p in MDCC-MSB1 cell proliferation and migration.

MATERIALS AND METHODS

Ethics statements
Animal experiments were specifically approved by the Animal Care and Use Committee of China Agricultural University (Approval ID: XXCB-20090209), and this study was carried out in strict accordance with the regulations and guidelines established by this committee. The animals were killed using T61 intravenously before dissection for sample collection. All efforts were made to minimize suffering.

Sample collection and experimental design
In our previous study, MDV challenge trial was conducted with 150 chickens from a White Leghorn specific pathogen-free line (BWEL) (Lian *et al.* 2010). A total of 100 1-d-old chickens was infected intraperitoneally with 2000 PFU of the MDV GA strain in CEF, and 50 chickens were injected with the same dosage of CEF cells (0.2 ml) as controls. The two groups were housed in separate isolators. The chickens were observed until 56 d postinfection (dpi). During this phase, the clinical signs of infected chickens were observed two to three times daily. Some chickens showed severe appetite loss, serious distress and depression, and impending death. These severely morbid chickens, and one to three age-matched noninfected chickens were killed using T61 intravenously (0.3 ml/kg) (Intervet, Ukkel, Belgium). The dead chickens were dissected, and their whole spleens and MD lymphoma in livers were collected. Eight MDV-infected tumorous spleens, eight MD lymphomas from liver, eight noninfected spleens, and eight noninfected livers collected during 30–56 dpi (Lian *et al.* 2012a) were used in this study. A schematic of the experimental design is shown in Supplemental Material, Figure S1. The binding sites of gga-miR-103-3p in the 3′-UTR of target genes were confirmed by luciferase reporter assay, and the expression of target genes in mRNA, and protein levels, were validated using real-time PCR and western blot analysis, respectively; moreover, the biological function of gga-miR-103-3p in cell proliferation and migration was investigated.

RNA isolation and real-time PCR for quantifying gga-miR-103-3p expression in tissue
Total RNA was isolated from tissue samples using a mirVana miRNA Isolation Kit (Ambion, Life Technologies, Carlsbad, CA), as described by the manufacturer, and reverse transcribed using a miRACLE cDNA Synthesis Kit (Genetimes Technology, Shanghai, China). Real-time PCR was performed on an ABI 7500 system (Applied Biosystems, Foster City, CA). A specific forward primer, and universal reverse primer, for gga-miR-103-3p, and a reference small noncoding RNA (chicken 5S rRNA), were designed and synthesized by Genetimes Technology, Inc (Table 1). Real-time PCR was performed using miRACLE qPCR miRNA Master Mix kit (Genetimes Technology). The optimum

■ **Table 2 Primers for wild-type and mutant-type vector construction**

Gene and Type	Direction	Sequence
CCNE1 wtUTR	Forward	CCGCTCGAGCTGTACGAACTGTTTACAG
	Reverse	TAAGCGGCCGCAAAGTATACGCCAAAATC
CCNE1 mut(75–81) UTR[a]	Forward	TTATGGAATACGACGCGGTGACATTCTAAAGCT
	Reverse	TGTCACCGCGTCGTATTCCATAATGGAGCAGGA
CCNE1 mut(248–254) UTR[a]	Forward	TGCTCCAATACGACGTATTGAGGGTGATGCTTG
	Reverse	CCTCAATACGTCGTATTGGAGCACTCTTCGGTG
CCNE1 mut(475–481) UTR[a]	Forward	TATTGTAATACGACGTATGTCTCTGTGTATCCA
	Reverse	GAGACATACGTCGTATTACAATAAAGAGTTTTT
TFDP2(1–1252) wtUTR[b]	Forward	CCGGCTCGAGAGACAGTGAAAAAAATGGATAC
	Reverse	TAAGCGGCCGCTATGAGAACCGTACATCTAC
TFDP2(1–1252)[b] mut(28–34) UTR[a]	Forward	AGACAGTGAAAAAAATGGATACACAAATACGACGACATATATATTCTTAATGG
	Reverse	TAAGCGGCCGCTATGAGAACCGTACATCTAC
TFDP2(5161–6415) wtUTR[b]	Forward	CCGGCTCGAGAGACAGTGAAAAAAATGGATAC
	Reverse	TAAGCGGCCGCTATGAGAACCGTACATCTAC
TFDP2(5161–6415)[b] mut(5609–5615) UTR[a]	Forward	ACTTTTTATACGACGACTTAAAGTTTGTAAACTT
	Reverse	ACTTTAAGTCGTCGTATAAAAAGTAATGTTTTTG
TFDP2(5161–6415)[b] mut(6254–6260) UTR[a]	Forward	TACTGAAATACGACGAAGCGGGAATTGTACATTG
	Reverse	TTCCCGCTTCGTCGTATTTCAGTAAACATGGAAT

wt, wild type; mut, mutant.
[a] Mutation position in 3′-UTR.
[b] Position in 3′-UTR.

thermal cycling parameters were 95° for 10 min, 40 cycles of 95° for 10 s, 60° for 20 s, 72° for 1 min, 95° for 15 s, 60° for 30 s, and 95° for 15 s. All experiments were run in triplicate. The expression of gga-miR-103-3p was measured using the $2^{-\Delta\Delta Ct}$ method.

Target genes prediction

The target genes of gga-miR-103-3p were predicted using the online tools TargetScan (http://www.targetscan.org) and miRDB (http://mirdb.org/miRDB/). Gene ontology (GO) analysis was conducted to screen the genes related to disease, immune system, cell cycle, cell proliferation, and cell migration by DAVID (Database for Annotation, Visualization and Integrated Discovery, http://david.abcc.ncifcrf.gov/).

Luciferase reporter assay

The human embryonic kidney 293T (HEK 293T) cell line was used to perform the luciferase reporter assay. Cells were grown in Dulbecco's modified Eagle's medium (DMEM) (Gibco, Life Technologies, Carlsbad, CA) supplemented with 10% fetal bovine serum (FBS) (Gibco). All cells were maintained at 37° in a humidified incubator containing 5% CO_2. The luciferase reporter vectors were constructed (RiboBio, Guangzhou, China). Briefly, fragments of 3′-UTR sequences covering the putative gga-miR-103-3p binding sites were amplified, and then inserted into pmiR-RB-REPORT luciferase reporter vectors to construct wild-type 3′-UTR vector. Mutant 3′-UTR vector was constructed by PCR amplification with wild-type 3′-UTR vector as template. The primers for wild-type (wt) and mutant-type (mut) vector were shown in Table 2. The CCNE1 wt UTR reporter and three mutant-type 3′-UTR reporters corresponding to three potential binding sites, including CCNE1 mut (75–81) UTR, CCNE1 mut (248-254) UTR, and CCNE1 mut (475-481) UTR, were constructed. Two wild luciferase reporters for TFDP2 gene were constructed because of the long sequence of its 3′-UTR region: TFDP2 wt (1–1252) UTR and TFDP2 wt (5161–6415) UTR. These two reporters have one and two binding sites for gga-miR-103-3p, respectively. These three reporters, TFDP2(1–1252) mut (28–34) UTR, TFDP2 (5161–6415) mut (5609–5615) UTR, and TFDP2 (5161–6415) mut (6254-6260) UTR, were constructed for detecting the real binding site. The gga-miR-103-3p mimics and mimics negative control (NC) were synthesized by GenePharma (Shanghai, China; Table 3). HEK 293T cells were plated into 96-well plates, and cultured 24 hr before cotransfection at 60% confluence. Then, pmiR-RB-Report luciferase reported vector containing wild type or mutant type were cotransfected with gga-miR-103-3p mimics, or NC, into HEK 293T cells using FuGENE HD transfection reagent (Promega, Madison, WI). Luciferase activity was measured 24 hr after cotransfection by the Dual-Luciferase Reporter Assay System (Promega) following the manufacturer's instruc-

tions. The results were expressed as relative luciferase activities (Renilla luciferase/Firefly luciferase) normalized against the mimics NC group. All experiments were performed in triplicate.

Gain/loss function study

The MD lymphoma cell line MDCC-MSB1 [provided by Dr. C. Itakura (Akiyama and Kato 1974; Goryo et al. 1987)] was cultured in RPMI-1640 medium (Gibco) with 10% FBS. All cells were maintained at 37° in a humidified incubator containing 5% CO_2. The gga-miR-103-3p mimics, mimics NC, gga-miR-103-3p inhibitor, and inhibitor NC were transfected into MDCC-MSB1 cells with FuGENE HD transfection reagent, respectively. Total RNA was isolated at 24 hr, 48 hr, and 72 hr after transfection, and real-time PCR was performed as described above for validating the expression of gga-miR-103-3p. To detect gene expression, total RNA was extracted from MDCC-MSB1 cells using E.Z.N.A. Total RNA Kit II (Omega, GA), and reverse transcribed into cDNA by EasyScript First-Strand cDNA Synthesis SuperMix (TransGen Biotech, Beijing, China). Each reaction was in a final volume of 15 μl, containing 1 μl of cDNA, 0.2 μl of each gene primer (100 nM, Table 4), and 1× PCR mix (Power SYBR Green PCR Master Mix, Applied Biosystems), and the optimum thermal cycling parameters included 95° for 10 min, 40 cycles of 95° for 10 s, 60° for 1 min, 95° for 15 s, 60° for 30 s, and 95° for 15 s. All experiments were run in triplicate. The expression of gga-miR-103-3p, and the two targets, were measured using the $2^{-\Delta\Delta Ct}$ method.

Western blot

MDCC-MSB1 cells were seeded into six-well plates, and transfected with gga-miR-103-3p mimics, mimics NC, gga-miR-103-3p inhibitor, and inhibitor NC, respectively. Proteins were isolated at 72 hr post transfection using radio immunoprecipitation assay (RIPA) lysis buffer with phenylmethanesulfonylfluoride (PMSF). The concentration of proteins was determined by the BAC assay (BCA Protein Assay Kit, Beyotime, Shanghai, China). Western blot was performed using standard methods (Blake et al. 1984; Dennis-Sykes et al. 1985). Proteins and protein marker (PageRuler Prestained Protein Ladder, Thermo Scientific, Life Technologies, Carlsbad, CA) were separated by 10% SDS-PAGE gels, and then transferred to polyvinylidene difluoride (PVDF) membranes. Membranes were blocked for 1 hr, and incubated overnight with Cyclin E Antibody (Novus Biologicals, Littleton, CO, 1:1000), Rabbit Anti-TFDP2 Polyclonal Antibody (Bioss Antibodies, Woburn, MA, 1:1000), and Actin antibody (Bayotime, Shanghai, China, 1:1000). After washing, the membranes were incubated for 1 hr with HRP-labeled Goat Anti-Rabbit IgG (H+L) (1:1000), HRP-labeled Goat Anti-Rabbit IgG (H+L) (1:1000), and HRP-labeled Goat Anti-Mouse IgG (H+L) (1:1000), respectively (Bayotime). Proteins were detected using BeyoECL Plus (Bayotime). The grayscale values of protein bands were analyzed using ImageJ. The grayscale value of CCNE1 or TFDP2 was standardized to that of ACTIN.
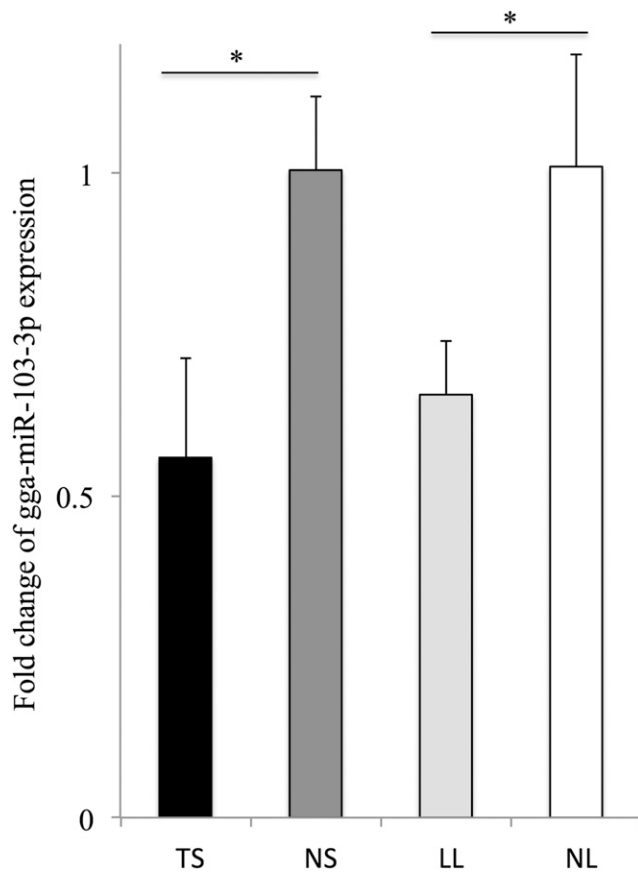
Figure 1 Differential expression of gga-miR-103-3p among tumorous spleen, noninfected spleen, MD lymphoma from liver, and noninfected liver. Results were measured using the $2^{-\Delta\Delta Ct}$ method. The fold change of TS was compared with that of NS, and NL was the control for LL. * $P < 0.05$. TS, tumorous spleen; NS, noninfected spleen; LL, MD lymphoma from liver; NL, noninfected liver.

Cell proliferation and migration assay

A total of 1×10^4 MDCC-MSB1 cells per well were seeded into 96-well plates, and transfected with gga-miR-103-3p mimics, mimics NC, gga-miR-103-3p inhibitor, and inhibitor NC, respectively. The CCK-8 (Cell Counting Kit-8, Beyotime) was added to each well at 24 hr, 48 hr, and 72 hr post transfection, and incubated at 37° for 2 hr. The absorbance at 450 nm was measured using the microplate spectrophotometer. All experiments were performed in triplicate.

The migration ability of MDCC-MSB1 cells was detected using Transwells (8 mm pore size, Corning Costar Corp, Corning, NY) at 48 hr after transfection. Transwells were put into the 24-well plates. A total of 1.5×10^4 cells/well were seeded in the upper chamber, and 500 µl of RPMI-1640 containing 20% FBS was added into the lower chambers. After incubating for 16 hr at 37° in a 5% CO_2 humidified incubator, the cells were counted under a microscope in three independent fields, with magnification of $\times$ 100. The mean of triplicate assays for each experimental condition was used. All experiments were performed in triplicate.

Data analysis

Data were expressed as the mean ± SD. The data were analyzed using a two-tailed Student's t-test, and the differences were considered to be statistically significant at $P < 0.05$.

RESULTS

Differential expression of gga-miR-103-3p between MDV-infected and noninfected groups

The expression of gga-miR-103-3p among tumorous spleen, MD lymphoma from liver, noninfected spleen, and noninfected liver, was detected by qPCR. The results showed that expression of gga-miR-103-3p was significantly downregulated in tumorous spleen and MD lymphoma from liver compared with the noninfected tissues (Figure 1).

Prediction and verification of gga-miR-103-3p target genes

In total, 236 and 316 target genes were predicted by TargetScan and miRDB, respectively. Fifty-six genes were predicted in both databases, which were used for GO analysis on the DAVID platform. The 56 common genes were clustered to different kinds of biological processes, including energy metabolism, ion transport, and cellular processes. Cyclin E1 (*CCNE1*), and transcription factor DP-2 (E2F dimerization partner 2) (*TFDP2*), the two genes with the highest prediction score in both TargetScan and miRDB, are linked with the cell cycle (KEGG Pathway: map 04110), and TFDP2 is involved in regulation of transcription (GO:0045449) (File S1). Referring to the results of GO analysis, and our previous microarray study (Lian *et al.* 2012a), *CCNE1* and *TFDP2* were chosen for further validation.

The luciferase reporter system was used to detect the interaction of miRNA and its predicted target genes. The results showed that relative luciferase activity of *CCNE1* wt UTR reporter was significantly inhibited by 40% when cotransfected with gga-miR-103-3p mimics compared with mimics NC (Figure 2B). The three mutant-type reporters, including *CCNE1* mut (75–81) UTR, *CCNE1* mut (248–254) UTR, and *CCNE1* mut (475–481) UTR reporter, were cotransfected with gga-miR-103-3p mimics, and mimics NC, respectively. The results showed that the relative luciferase activities of *CCNE1* mut (248–254) UTR reporter transfected with gga-miR-103-3p mimics was significantly decreased compared with mimic NC. *CCNE1* mut (75–81) UTR and *CCNE1* mut (475–481) UTR had no significant change, but the relative luciferase activities of *CCNE1* (475–481) UTR displayed a downtrend when this reporter was cotransfected with gga-miR-103-3p mimics (Figure 2B). Taken together, the results demonstrate strongly that the *CCNE1* (248–254) UTR was not the binding site of gga-miR-103-3p. The *CCNE1* (75–81) UTR and *CCNE1* (475–481) UTR could bind gga-miR-103-3p, and the *CCNE1* (75–81) UTR was the primary binding site of gga-miR-103-3p.

The relative luciferase activities of *TFDP2* wt (1–1252) UTR and *TFDP2* wt (5161–6415) UTR reporters cotransfected with gga-miR-103-3p mimics were both significantly decreased (Figure 2D). However, the relative luciferase activities of the three mutant-type luciferase reporters exhibited no significant change after cotransfection (Figure 2D). These results suggest that gga-miR-103-3p could bind to three sites in the target *TFDP2* mRNA. Overall, *CCNE1* and *TFDP2* are the two candidate target genes for gga-miR-103-3p.

The RNA expression of gga-miR-103-3p, *CCNE1*, and *TFDP2* in MDCC-MSB1 cells was examined at 24 hr, 48 hr, and 72 hr after transfecting gga-miR-103-3p mimics, mimics NC, gga-miR-103-3p inhibitor, and inhibitor NC, respectively. As shown in Figure 3, the expression level of gga-miR-103-3p was significantly higher in the gga-miR-103-3p mimics group, and lower in the gga-miR-103-3p inhibitor transfection group than that in corresponding negative control,
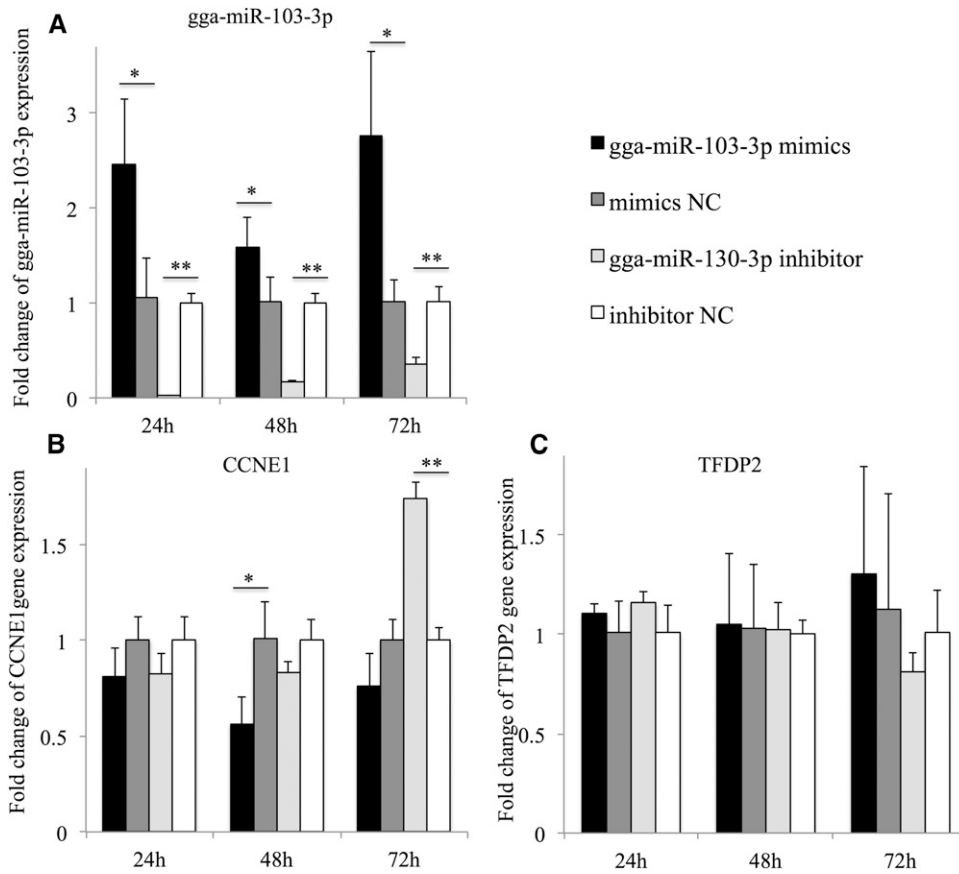
Figure 2 Luciferase reporter assay. (A) Nucleotide sequences of *CCNE1* wild type and mutant in the 3′-untranslated region (3′-UTR). Three potential binding sites were marked in bold italic. (B) The relative luciferase activities of *CCNE1* wild type and mutant reporters normalized against mimics NC. (C) Nucleotide sequences of *TFDP2* wild type and mutant in the 3′-UTR. Three potential binding sites were marked with bold italic. (D) The relative luciferase activities of *TFDP2* wild and mutant reporters normalized against mimics NC. Two wild luciferase reporters [*TFDP2* wt (1–1252) UTR and *TFDP2* wt (5161–6415) UTR] for the *TFDP2* gene were constructed because of its long 3′-UTR region. * $P < 0.05$.

respectively (Figure 3A). On the contrary, expression of *CCNE1* was significantly lower at 48 hr after transfection with gga-miR-103-3p mimics compared with the mimics NC group. At 24 hr and 72 hr, the expression of *CCNE1* in the mimics groups exhibited no marked change, but there was a visible downward trend. The expression of *CCNE1* at 72 hr after transfecting MDCC-MSB1 cells with gga-miR-103-3p inhibitor was notably increased compared with the inhibitor NC group, which indirectly indicated that gga-miR-103-3p could bind with *CCNE1* (Figure 3B). However, there was no obvious change in *TFDP2* mRNA level after transfection (Figure 3C). The results demonstrated that gga-miR-103-3p could interfere with expression of *CCNE1* mRNA, but did not regulate *TFDP2* mRNA expression.

The protein expression levels of *CCNE1* and *TFDP2* were detected in MDCC-MSB1 cells at 72 hr after transfection with gga-miR-103-3p mimics, mimics NC, gga-miR-103-3p inhibitor, and inhibitor NC, respectively. The results showed that the protein levels of *CCNE1* and

TFDP2 were significantly reduced after transfection with gga-miR-103-3p mimics compared with mimics NC, and the relative protein expression of these two genes in gga-miR-103-3p inhibitor groups were notably increased compared to inhibitor NC groups, respectively (Figure 4). Results of target mRNA expression and western blot assay indicated that gga-miR-103-3p regulated *CCNE1* gene expression at both mRNA and protein levels. However, gga-miR-103-3p could modulate *TFDP2* at the protein but not the mRNA level.

The effects of gga-miR-103-3p on cell proliferation and migration

To explore the role played by gga-miR-103-3p in MDCC-MSB1 cells, we performed cell proliferation and migration assays after overexpressing or interfering with gga-miR-103-3p. The increasing cell viability at various time points indicated that cell proliferation increased over time. However, the cell viability exhibited no obvious change at 24 hr, 48 hr,

Figure 3 Expression of (A) gga-miR-103-3p, (B) *CCNE1*, and (C) *TFDP2* at 24 hr, 48 hr, and 72 hr. Results showed the fold change of expression using the $2^{-\Delta\Delta Ct}$ method. Chicken 5S rRNA and *GAPDH* were the endogenous reference for gga-miR-103-3p and the two target genes, respectively. The gga-miR-103-3p mimics group was compared with mimics NC group, and inhibitor NC group was the control for gga-miR-103-3p inhibitor group. * $P < 0.05$, ** $P < 0.01$.

and 72 hr in gga-miR-103-3p mimics or gga-miR-103-3p inhibitor groups, compared with the corresponding NC group (Figure 5A). This suggested that gga-miR-103-3p could not influence MDCC-MSB1 cell proliferation. As shown in Figure 5B, the migrated cell number in the gga-miR-103-3p mimics transfection group was notably decreased compared with the mimics NC group, suggesting that overexpression of gga-miR-103-3p could inhibit MDCC-MSB1 cell migration at 48 h. Collectively, gga-miR-103-3p could suppress MDCC-MSB1 cell migration, but has no obvious effects on its proliferation.

DISCUSSION

MicroRNAs are associated with a variety of diseases, including cancers and oncosis (Chen *et al.* 2008). It was reported that miR-103 was differentially expressed in lung cancer (Garofalo *et al.* 2012), colorectal cancer (Chen *et al.* 2012), human gastric carcinoma (Zhang *et al.* 2015),

and breast cancer (Kleivi Sahlberg *et al.* 2015). Although, miR-103 has been investigated extensively in mammalian diseases, studies on gga-miR-103 in chickens are still limited. In recent years, only a few studies on chicken gga-miR-103 have been reported, including deep sequencing in chicken preadipocytes (Yao *et al.* 2011), hypothalamus tissue (Sun *et al.* 2012), chromium metabolism (Pan *et al.* 2013), abdominal fatness (Wang *et al.* 2015), and abdominal adipose tissues (Huang *et al.* 2015). As for MD, it was reported that gga-miR-103-3p was expressed differentially between MDV-infected and uninfected CEF cells (Burnside *et al.* 2008). In MDV-infected chickens of line 7_2 (MD susceptible line), the expression of gga-miR-103 was significantly downregulated compared with noninfected chickens at 21 dpi (Tian *et al.* 2012). Our results showed that gga-miR-103-3p was greatly decreased in MDV-infected tissues, which is consistent with the previous studies (Burnside *et al.* 2008; Tian *et al.* 2012).
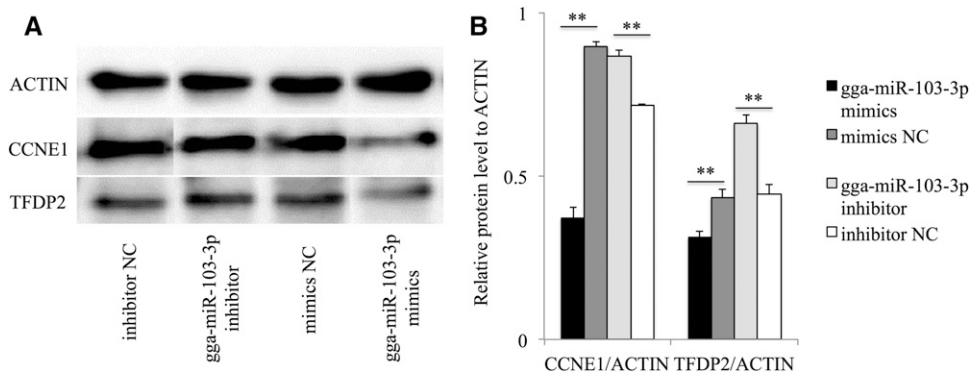

Figure 4 Protein expression levels of *CCNE1*, *TFDP2*, and *ACTIN* at 72 hr in MDCC-MSB1 cells after transfecting gga-miR-103-3p mimics, mimics NC, gga-miR-103-3p inhibitor, and inhibitor NC, respectively. (A) Results of western blot assay. (B) The ratio of gray scale values of *CCNE1* and *TFDP2* to that of *ACTIN*. ** $P < 0.01$.
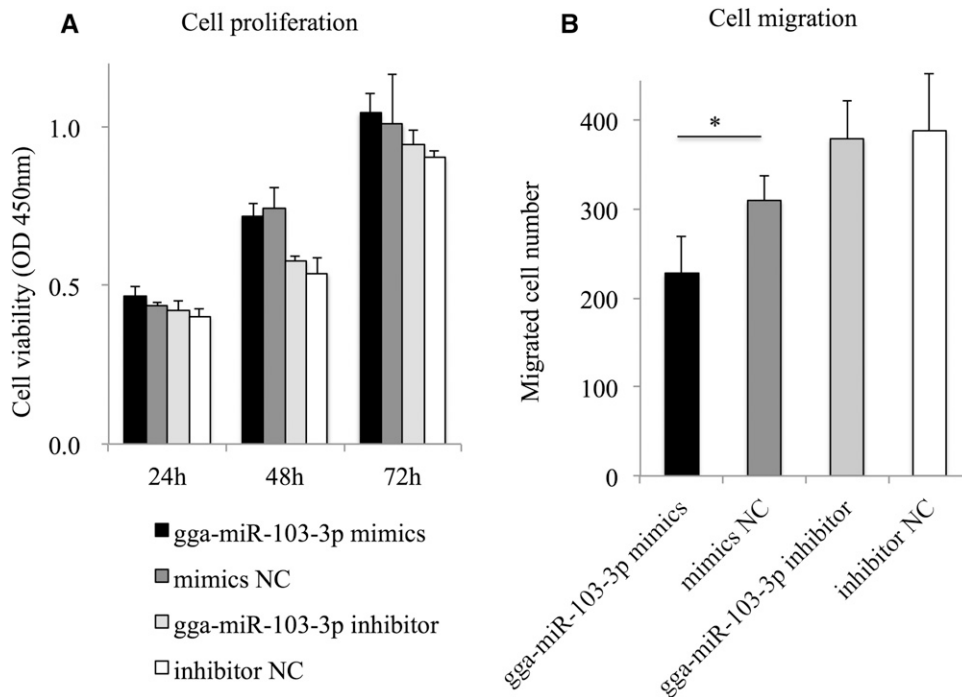
A Cell proliferation

B Cell migration

Figure 5 Effects of gga-miR-103-3p on cell proliferation and migration of Marek's disease lymphoma cell line (MDCC-MSB1) cells. (A) Cell viability of MDCC-MSB1 cells after transfection with gga-miR-103-3p mimics, mimics NC, gga-miR-103-3p inhibitor, and inhibitor NC, respectively. OD, optical density. (B) The number of migrated MDCC-MSB1 cells at 48 hr after transfection with gga-miR-103-3p mimics, mimics NC, gga-miR-103-3p inhibitor, and inhibitor, respectively. Cell number is the mean of triplicate assays for each experimental condition. * $P < 0.05$.

Several studies have shown that miR-103 is involved in cancers, and in regulated cell proliferation and migration. A vital molecular relationship between miR-103 and *PER3* (period circadian clock 3) in human colorectal cancer (CRC) cell lines was confirmed. The proliferation and migration of CRC cells could be regulated by miR-103 (Hong *et al.* 2014). MiR-103/107 overexpression or *CDK5R1* [cyclin-dependent kinase 5, regulatory subunit 1 (p35)] silencing caused a reduction in SK-N-BE migration ability (Moncini *et al.* 2011). Our results suggested that gga-miR-103-3p suppressed cell migration in the MDCC-MSB1 cell line.

miRNAs play critical roles in gene regulatory networks. An individual miRNA can target hundreds or thousands of different mRNAs; meanwhile, an individual gene can be coordinately suppressed by multiple various miRNAs (Krek *et al.* 2005; Friedman *et al.* 2009). The miR-103 family has been found in 23 species (Griffiths-Jones 2004; Griffiths-Jones *et al.* 2006). A total of 257 conserved sites, and 79 poorly conserved sites, were predicted using TargetScan, and the seed regions, which aligned to mRNA 3'-UTR of targets, were the same in different species, suggesting that the targets were highly conserved among human, chicken, and some other species (http://www.targetscan.org/cgi-bin/targetscan/vert_61/targetscan.cgi?mirg=gga-miR-103). Considering the results of TargetScan, miRDB, and GO analysis, we selected two target genes, *CCNE1* and *TFDP2*, for further validation. The product of the *CCNE1* gene forms a complex with CDK2 (cyclin-dependent kinase 2), and functions as a regulatory subunit, which is required for cell cycle G1/S transition (Ekholm and Reed 2000; Mazumder *et al.* 2004; Sherr 2000; Sherr and Roberts 1995). Overexpression of this gene can cause chromosome instability in many tumors; thus, it may contribute to tumorigenesis. The expression level of *CCNE1* begins to rise in mid-G1 phase, peaks during late G1, and declines around the G1/S transition. So the timing of its expression level plays a critical role in initiation of DNA replication as well as chromatin remodeling during tumorigenesis (Hu *et al.* 2014). *CCNE1* is the target gene of miR-15/16 in human lung cancer (Bandi and Vassella 2011) and glioblastoma (Xia *et al.* 2009) during tumorigenesis (http://www.kegg.jp/kegg-bin/show_pathway?hsa05206+898). From the point

of view of cancer or tumor research, it was reported that miR-103 is part of the G1/S transition regulatory network, by targeting *CCNE1*, *CDK2*, and *CREB1* (cAMP responsive element binding protein 1) during IGF-1 simulated proliferation in mouse crypt cells (Liao and Lonnerdal 2010). miR-107, as a paralog of miR-103, was identified in human nonsmall cell lung cancer, and the potential target *CCNE1* was downregulated by transfection with miR-107 (Takahashi *et al.* 2009). In this study, we identified a binding site of gga-miR-103-3p in the 3'UTR of *CCNE1*, and verified that *CCNE1* was a target gene of gga-miR-103-3p.

The *TFDP2* gene (E2F/DP2) belongs to the transcription factor dimerization partner (DP) family, and its encoded protein forms heterodimers with the E2F transcription factor, resulting in transcriptional activation of cell cycle regulated genes (Wu *et al.* 1995; Zhang *et al.* 1997). E2F complexes can be broadly classified into two subgroups: "activating" E2Fs (E2F1, E2F2, and E2F3), and "repressive" E2Fs (E2F4, E2F5, and E2F6) (Trimarchi and Lees 2002). Studies have suggested that E2F1 is the target gene of miR-20a (Sylvestre *et al.* 2007), miR-106b (Ambs *et al.* 2008), and miR-330 (Lee *et al.* 2009) in prostate cancer. These two target genes are involved in the cell cycle pathway (KEGG Pathway: map 04110), and affect cell cycle progression from G1 phase to S phase. Therefore, aberrant expressions of these two genes may disturb the normal cell cycle, and further cause tumorigenesis (http://www.genome.jp/kegg-bin/show_pathway?map04110). Meanwhile, the Cyclin E family and E2F factors participate in the pathways in cancer (KEGG Pathway: ko 05200), and can affect cell proliferation indirectly (http://www.genome.jp/kegg-bin/show_pathway?map05200). Additionally, *TFDP2* could be targeted by miR-122, which inhibits *c-Myc* transcription in hepatocellular cancer indirectly (B. Wang *et al.* 2014). Here, we verified that TFDP2 was another target gene of gga-miR-103-3p by luciferase reporter assay and western blot assay.

In summary, we found that gga-miR-103-3p was downregulated in MDV-infected tissues, and it inhibits cell migration in MDCC-MSB1 cell lines. The two target genes *CCNE1* and *TPDP2* were identified. The effective binding sites of gga-miR-103-3p in the 3'-UTR of *CCNE1* and *TFDP2* mRNA were confirmed. Gga-miR-103-3p

could suppress *CCNE1* gene expression at both mRNA and protein levels, while the *TPDP2* gene was regulated by gga-miR-103-3p at the protein but not mRNA level. Gga-miR-103-3p, working together with its targets, may play a potential role in MDV tumorigenesis.

ACKNOWLEDGMENTS

LITERATURE CITED

Akiyama, Y., and S. Kato, 1974   Two cell lines from lymphomas of Marek's disease. Biken J. 17(3): 105–116.

Ambs, S., R. L. Prueitt, M. Yi, R. S. Hudson, T. M. Howe *et al.*, 2008   Genomic profiling of microRNA and messenger RNA reveals deregulated microRNA expression in prostate cancer. Cancer Res. 68(15): 6162–6170.

Bandi, N., and E. Vassella, 2011   miR-34a and miR-15a/16 are co-regulated in non-small cell lung cancer and control cell cycle progression in a synergistic and Rb-dependent manner. Mol. Cancer 10: 55.

Bartel, D. P., 2009   MicroRNAs: target recognition and regulatory functions. Cell 136(2): 215–233.

Blake, M. S., K. H. Johnston, G. J. Russell-Jones, and E. C. Gotschlich, 1984   A rapid, sensitive method for detection of alkaline phosphatase-conjugated anti-antibody on Western blots. Anal. Biochem. 136(1): 175–179.

Burnside, J., and R. Morgan, 2011   Emerging roles of chicken and viral microRNAs in avian disease. BMC Proc. 5(Suppl 4): S2.

Burnside, J., E. Bernberg, A. Anderson, C. Lu, B. C. Meyers *et al.*, 2006   Marek's disease virus encodes microRNAs that map to meq and the latency-associated transcript. J. Virol. 80(17): 8778–8786.

Burnside, J., M. Ouyang, A. Anderson, E. Bernberg, C. Lu *et al.*, 2008   Deep sequencing of chicken microRNAs. BMC Genomics 9: 185.

Calin, G. A., and C. M. Croce, 2006   MicroRNA signatures in human cancers. Nat. Rev. Cancer 6(11): 857–866.

Calnek, B. W., 1986   Marek's disease—a model for herpesvirus oncology. Crit. Rev. Microbiol. 12(4): 293–320.

Calnek, B. W., 2001   Pathogenesis of Marek's disease virus infection. Curr. Top. Microbiol. Immunol. 255: 25–55.

Chen, H. Y., Y. M. Lin, H. C. Chung, Y. D. Lang, C. J. Lin *et al.*, 2012   miR-103/107 promote metastasis of colorectal cancer by targeting the metastasis suppressors DAPK and KLF4. Cancer Res. 72(14): 3631–3641.

Chen, X., Y. Ba, L. Ma, X. Cai, Y. Yin *et al.*, 2008   Characterization of microRNAs in serum: a novel class of biomarkers for diagnosis of cancer and other diseases. Cell Res. 18(10): 997–1006.

Chi, J. Q., M. Teng, Z. H. Yu, H. Xu, J. W. Su *et al.*, 2015   Marek's disease virus-encoded analog of microRNA-155 activates the oncogene c-Myc by targeting LTBP1 and suppressing the TGF-beta signaling pathway. Virology 476: 72–84.

Dennis-Sykes, C. A., W. J. Miller, and W. J. McAleer, 1985   A quantitative western blot method for protein measurement. J. Biol. Stand. 13(4): 309–314.

Ekholm, S. V., and S. I. Reed, 2000   Regulation of G(1) cyclin-dependent kinases in the mammalian cell cycle. Curr. Opin. Cell Biol. 12(6): 676–684.

Farazi, T. A., J. I. Hoell, P. Morozov, and T. Tuschl, 2013   MicroRNAs in human cancer. Adv. Exp. Med. Biol. 774: 1–20.

Friedman, R. C., K. K. H. Farh, C. B. Burge, and D. P. Bartel, 2009   Most mammalian mRNAs are conserved targets of microRNAs. Genome Res. 19(1): 92–105.

Garofalo, M., G. Romano, G. Di Leva, G. Nuovo, Y. J. Jeon *et al.*, 2012   EGFR and MET receptor tyrosine kinase-altered microRNA expression induces tumorigenesis and gefitinib resistance in lung cancers. Nat. Med. 18(1): 74–82.

Gennart, I., D. Coupeau, S. Pejakovic, S. Laurent, D. Rasschaert *et al.*, 2015   Marek's disease: genetic regulation of gallid herpesvirus 2 infection and latency. Vet. J. 205(3): 339–348.

Gimeno, I. M., 2008   Marek's disease vaccines: a solution for today but a worry for tomorrow? Vaccine 26(Suppl 3): C31–C41.

Goryo, M., T. Suwa, S. Matsumoto, T. Umemura, and C. Itakura, 1987   Serial propagation and purification of chicken anaemia agent in MDCC-MSB1 cell line. Avian Pathol. 16(1): 149–163.

Griffiths-Jones, S., 2004   The microRNA registry. Nucleic Acids Res. 32 (Database issue): D109–D111.

Griffiths-Jones, S., R. J. Grocock, S. van Dongen, A. Bateman, and A. J. Enright, 2006   miRBase: microRNA sequences, targets and gene nomenclature. Nucleic Acids Res. 34(Database issue): D140–D144.

Han, W., J. M. Zou, K. H. Wang, Y. J. Su, Y. F. Zhu *et al.*, 2015   High-throughput sequencing reveals hypothalamic microRNAs as novel partners involved in timing the rapid development of chicken (*Gallus gallus*) gonads. PLoS One 10(6): e0129738.

Hicks, J. A., and H. C. Liu, 2013   Current state of Marek's disease virus microRNA research. Avian Dis. 57(2, Suppl) 332–339.

Hong, Z., Z. Feng, Z. Sai, and S. Tao, 2014   PER3, a novel target of miR-103, plays a suppressive role in colorectal cancer in vitro. BMB Rep. 47(9): 500–505.

Hu, W., Y. A. Nevzorova, U. Haas, N. Moro, P. Sicinski *et al.*, 2014   Concurrent deletion of cyclin E1 and cyclin-dependent kinase 2 in hepatocytes inhibits DNA replication and liver regeneration in mice. Hepatology 59(2): 651–660.

Huang, H. Y., R. R. Liu, G. P. Zhao, Q. H. Li, M. Q. Zheng *et al.*, 2015   Integrated analysis of microRNA and mRNA expression profiles in abdominal adipose tissues in chickens. Sci. Rep. 5: 16132.

Iorio, M. V., and C. M. Croce, 2012   microRNA involvement in human cancer. Carcinogenesis 33(6): 1126–1133.

Kang, L., X. Cui, Y. Zhang, C. Yang, and Y. Jiang, 2013   Identification of miRNAs associated with sexual maturity in chicken ovary by Illumina small RNA deep sequencing. BMC Genomics 14: 352.

Kleivi Sahlberg, K., G. Bottai, B. Naume, B. Burwinkel, G. A. Calin *et al.*, 2015   A serum microRNA signature predicts tumor relapse and survival in triple-negative breast cancer patients. Clin. Cancer Res. 21(5): 1207–1214.

Krek, A., D. Grun, M. N. Poy, R. Wolf, L. Rosenberg *et al.*, 2005   Combinatorial microRNA target predictions. Nat. Genet. 37(5): 495–500.

Lee, K. H., Y. L. Chen, S. D. Yeh, M. Hsiao, J. T. Lin *et al.*, 2009   MicroRNA-330 acts as tumor suppressor and induces apoptosis of prostate cancer cells through E2F1-mediated suppression of Akt phosphorylation. Oncogene 28(38): 3360–3370.

Li, H., G. R. Sun, S. J. Lv, Y. Wei, R. L. Han *et al.*, 2012   Association study of polymorphisms inside the miR-1657 seed region with chicken growth and meat traits. Br. Poult. Sci. 53(6): 770–776.

Li, H., G. R. Sun, Y. D. Tian, R. L. Han, G. X. Li *et al.*, 2013   MicroRNAs-1614–3p gene seed region polymorphisms and association analysis with chicken production traits. J. Appl. Genet. 54(2): 209–213.

Li, X., L. Lian, D. Zhang, L. Qu, and N. Yang, 2014   gga-miR-26a targets NEK6 and suppresses Marek's disease lymphoma cell proliferation. Poult. Sci. 93(5): 1097–1105.

Li, Z. J., Y. P. Zhang, Y. Li, H. W. Zheng, Y. S. Zheng *et al.*, 2014   Distinct expression pattern of miRNAs in Marek's disease virus infected-chicken splenic tumors and non-tumorous spleen tissues. Res. Vet. Sci. 97(1): 156–161.

Lian, L., L. J. Qu, J. X. Zheng, C. J. Liu, Y. P. Zhang *et al.*, 2010   Expression profiles of genes within a subregion of chicken major histocompatibility complex B in spleen after Marek's disease virus infection. Poult. Sci. 89 (10): 2123–2129.

G3·Genes | Genomes | Genetics

Lian, L., L. Qu, Y. Chen, S. J. Lamont, and N. Yang, 2012a A systematic analysis of miRNA transcriptome in Marek's disease virus-induced lymphoma reveals novel and differentially expressed miRNAs. PLoS One 7(11): e51003.

Lian, L., L. J. Qu, H. Y. Sun, Y. M. Chen, S. J. Lamont et al., 2012b Gene expression analysis of host spleen responses to Marek's disease virus infection at late tumor transformation phase. Poult. Sci. 91(9): 2130–2138.

Lian, L., X. Li, C. Zhao, B. Han, L. Qu et al., 2015 Chicken gga-miR-181a targets MYBL1 and shows an inhibitory effect on proliferation of Marek's disease virus-transformed lymphoid cell line. Poult. Sci. 94(11): 2616–2621.

Liao, Y. L., and B. Lonnerdal, 2010 Global microRNA characterization reveals that miR-103 is involved in IGF-1 stimulated mouse intestinal cell proliferation. PLoS One 5(9): e12976.

Lin, S., H. Li, H. Mu, W. Luo, Y. Li et al., 2012 Let-7b regulates the expression of the growth hormone receptor gene in deletion-type dwarf chickens. BMC Genomics 13: 306.

Lu, J., G. Getz, E. A. Miska, E. Alvarez-Saavedra, J. Lamb et al., 2005 MicroRNA expression profiles classify human cancers. Nature 435 (7043): 834–838.

Luo, J., A. J. Sun, M. Teng, H. Zhou, Z. Z. Cui et al., 2011 Expression profiles of microRNAs encoded by the oncogenic Marek's disease virus reveal two distinct expression patterns in vivo during different phases of disease. J. Gen. Virol. 92(Pt 3): 608–620.

Mazumder, S., E. L. DuPre, and A. Almasan, 2004 A dual role of Cyclin E in cell proliferation and apotosis may provide a target for cancer therapy. Curr. Cancer Drug Targets 4(1): 65–75.

Moncini, S., A. Salvi, P. Zuccotti, G. Viero, A. Quattrone et al., 2011 The role of miR-103 and miR-107 in regulation of CDK5R1 expression and in cellular migration. PLoS One 6(5): e20038.

Morgan, R., A. Anderson, E. Bernberg, S. Kamboj, E. Huang et al., 2008 Sequence conservation and differential expression of Marek's disease virus microRNAs. J. Virol. 82(24): 12213–12220.

Pan, Y. Z., S. G. Wu, H. C. Dai, H. J. Zhang, H. Y. Yue et al., 2013 Solexa sequencing of microRNAs on chromium metabolism in broiler chicks. J. Nutrigenet. Nutrigenomics 6(3): 137–153.

Rengaraj, D., T. S. Park, S. I. Lee, B. R. Lee, B. K. Han et al., 2013 Regulation of glucose phosphate isomerase by the 3′UTR-specific miRNAs miR-302b and miR-17–5p in chicken primordial germ cells. Biol. Reprod. 89(2): 33.

Sherr, C. J., 2000 The Pezcoller lecture: cancer cell cycles revisited. Cancer Res. 60(14): 3689–3695.

Sherr, C. J., and J. M. Roberts, 1995 Inhibitors of mammalian G1 cyclin-dependent kinases. Genes Dev. 9(10): 1149–1163.

Sun, G. R., M. Li, G. X. Li, Y. D. Tian, R. L. Han et al., 2012 Identification and abundance of miRNA in chicken hypothalamus tissue determined by Solexa sequencing. Genet. Mol. Res. 11(4): 4682–4694.

Sylvestre, Y., V. De Guire, E. Querido, U. K. Mukhopadhyay, V. Bourdeau et al., 2007 An E2F/miR-20a autoregulatory feedback loop. J. Biol. Chem. 282(4): 2135–2143.

Takahashi, Y., A. R. Forrest, E. Maeno, T. Hashimoto, C. O. Daub et al., 2009 MiR-107 and MiR-185 can induce cell cycle arrest in human non small cell lung cancer cell lines. PLoS One 4(8): e6677.

Teng, M., Z. H. Yu, A. J. Sun, Y. J. Min, J. Q. Chi et al., 2015 The significance of the individual Meq-clustered miRNAs of Marek's disease virus in oncogenesis. J. Gen. Virol. 96(Pt 3): 637–649.

Tian, F., J. Luo, H. Zhang, S. Chang, and J. Song, 2012 MiRNA expression signatures induced by Marek's disease virus infection in chickens. Genomics 99(3): 152–159.

Trimarchi, J. M., and J. A. Lees, 2002 Sibling rivalry in the E2F family. Nat. Rev. Mol. Cell Biol. 3(1): 11–20.

Wang, B., S. H. Hsu, X. Wang, H. Kutay, H. K. Bid et al., 2014 Reciprocal regulation of microRNA-122 and c-Myc in hepatocellular cancer: role of E2F1 and transcription factor dimerization partner 2. Hepatology 59(2): 555–566.

Wang, Q., Y. Gao, X. Ji, X. Qi, L. Qin et al., 2013 Differential expression of microRNAs in avian leukosis virus subgroup J-induced tumors. Vet. Microbiol. 162(1): 232–238.

Wang, W., Z. Q. Du, B. Cheng, Y. Wang, J. Yao et al., 2015 Expression profiling of preadipocyte microRNAs by deep sequencing on chicken lines divergently selected for abdominal fatness. PLoS One 10(2): e0117843.

Wang, X., L. Yang, H. Wang, F. Shao, J. Yu et al., 2014 Growth hormone-regulated mRNAs and miRNAs in chicken hepatocytes. PLoS One 9(11): e112896.

Wang, Z., Y. Li, D. Kong, A. Ahmad, S. Banerjee et al., 2010 Cross-talk between miRNA and Notch signaling pathways in tumor development and progression. Cancer Lett. 292(2): 141–148.

Wu, C. L., L. R. Zukerberg, C. Ngwu, E. Harlow, and J. A. Lees, 1995 In vivo association of E2F and DP family proteins. Mol. Cell. Biol. 15(5): 2536–2546.

Xia, H., Y. Qi, S. S. Ng, X. Chen, S. Chen et al., 2009 MicroRNA-15b regulates cell cycle progression by targeting cyclins in glioma cells. Biochem. Biophys. Res. Commun. 380(2): 205–210.

Xu, S., C. Xue, J. Li, Y. Bi, and Y. Cao, 2011 Marek's disease virus type 1 microRNA miR-M3 suppresses cisplatin-induced apoptosis by targeting Smad2 of the transforming growth factor beta signal pathway. J. Virol. 85(1): 276–285.

Yao, J., Y. Wang, W. Wang, N. Wang, and H. Li, 2011 Solexa sequencing analysis of chicken pre-adipocyte microRNAs. Biosci. Biotechnol. Biochem. 75(1): 54–61.

Yu, Z. H., M. Teng, A. J. Sun, L. L. Yu, B. Hu et al., 2014 Virus-encoded miR-155 ortholog is an important potential regulator but not essential for the development of lymphomas induced by very virulent Marek's disease virus. Virology 448: 55–64.

Zhang, S. P., S. Y. Li, W. Chen, W. W. Lu, and Y. Q. Huang, 2013 A single-nucleotide polymorphism in the 3′ untranslated region of the LPIN1 gene and association analysis with performance traits in chicken. Br. Poult. Sci. 54(3): 312–318.

Zhang, Y., X. Qu, C. Li, Y. Fan, X. Che et al., 2015 miR-103/107 modulates multidrug resistance in human gastric carcinoma by downregulating Cav-1. Tumour Biol. 36(4): 2277–2285.

Zhang, Y. H., V. S. Venkatraj, S. G. Fischer, D. Warburton, and S. P. Chellappan, 1997 Genomic cloning and chromosomal assignment of the E2F dimerization partner TFDP gene family. Genomics 39(1): 95–98.

Zhao, Y., Y. Yao, H. Xu, L. Lambeth, L. P. Smith et al., 2009 A functional microRNA-155 ortholog encoded by the oncogenic Marek's disease virus. J. Virol. 83(1): 489–492.

Zhao, Y., H. Xu, Y. Yao, L. P. Smith, L. Kgosana et al., 2011 Critical role of the virus-encoded microRNA-155 ortholog in the induction of Marek's disease lymphomas. PLoS Pathog. 7(2): e1001305.

Communicating editor: D. W. Threadgill